Chinese Chemical Letters 33 (2022) 703–713

Contents lists available at ScienceDirect

Chinese Chemical Letters

journal homepage: www.elsevier.com/locate/cclet

Graphene-based hemostatic sponge

Bingxin Wu[1], Fanglin Du[1], Wenjing A, Guofeng Li*, Xing Wang*

State Key Laboratory of Organic-Inorganic Composites, Beijing Laboratory of Biomedical Materials, Beijing University of Chemical Technology Beijing, 100029, China

ARTICLE INFO

Article history:
Received 9 April 2021
Revised 20 May 2021
Accepted 9 June 2021
Available online 16 June 2021

Keywords:
Graphene
Hemostatic sponge
Composite materials
Synergistic effect
Coagulation stimulation

ABSTRACT

Graphene-based sponge is a novel hemostatic material prepared by chemical cross-link of graphene oxide. It has a fast fluid absorption capacity to quickly absorb blood from wounds, activate clotting pathways, and achieve rapid hemostasis. In addition, graphene-based sponge is also a good platform carrier. It can be prepared by organic cross-linking, compounding with inorganic clay, and adding bioactive factors to enhance coagulation stimulation. By these methods, the hemostatic performance of the sponge is further improved, which shows great potential for application in the field of trauma hemostasis. This article reviews the research progress of graphene-based sponges from three different preparation strategies (organic cross-linking, inorganic compounding and adding bioactive factor), summarizes their hemostatic mechanisms, and prospects the development of graphene-based hemostatic sponges.

1. Introduction

Uncontrolled bleeding is a major cause of traumatic death [1], especially on the battlefield, in emergencies and medical operations [2]. Meanwhile, massive bleeding loss causes serious pathological consequences and complications, such as metabolic and cellular dysfunction [3], hemorrhagic shock, coagulation and acidosis, which directly increase physical morbidity and mortality [4]. Therefore, the use of effective hemostats is essential for life-saving and postoperative recovery [5,6].

At present, an increasing number of hemostatic materials have been developed, mainly including hemostatic sponge, powder, forcep, gauze, hydrogel (Fig. 1). They can be divided into three categories: (1) Organic hemostatic materials, such as natural polysaccharides, recombinant factor VIIa, thrombin and fibrin [6-9]. Such materials are characterized by good biocompatibility and do not require debridement. Yang *et al.* [6] reviewed the research progress and hemostatic mechanisms of polysaccharide hemostatic materials. (2) Inorganic hemostatic materials, such as zeolite, kaolin, montmorillonite, mesoporous silica gel, alum [10-12]. The characteristics of inorganic hemostatic materials are high efficiency, stability and easy operation. Sara [11] reviewed the most commonly used inorganic hemostatic agents, discussed their hemostatic effects and structural characteristics. (3) Composite hemostatic materials, such as chitosan/starch composite sponge, polyvinyl alcohol (PVA)/sodium alginate (SA) composite foam [13]. They eliminate the shortcomings of a single hemostatic material by compounding two or more organic and inorganic hemostatic materials. The hemostatic efficiency and biological safety of materials could be further improved.

Graphene, as a two-dimensional (2D) atomic crystal, has outstanding electrical, thermal and mechanical properties. Due to its flexible chemical functionality, it is an excellent filler for developing composite materials. Therefore, it is considered as a “magic material” and has received much attention. On the one hand, graphene-based composites can be prepared by loading different functional molecules on graphene sheets, showing obvious multifunctional effects [14-19], which are widely used in biomedical fields, such as biosensors, biological imaging, drug delivery, antibacterial materials and tissue engineering [20-30]. On the other hand, the three-dimensional (3D) graphene macrostructures [31-35] have the advantages of low density, high porosity, high specific surface area and excellent electrochemical properties. They can be used to manufacture sponge, foam, hydrogel, film and other forms. It is also widely used for conductive sensing [36,37], building insulation [31,38], absorbing organic solvents, energy storage [39] and other fields. Graphene-based materials exhibit extraordinary properties, which have become a hot topic nowadays, providing a great impetus and commercial potential for materials development and nanotechnology innovation. Previous studies have shown the potential of graphene-based materials for hemostatic applications.

* Corresponding authors.
E-mail addresses: chase.lg@163.com (G. Li), wangxing@mail.buct.edu.cn (X. Wang).
[1] These authors contributed equally to this work.

https://doi.org/10.1016/j.cclet.2021.06.029
1001-8417/

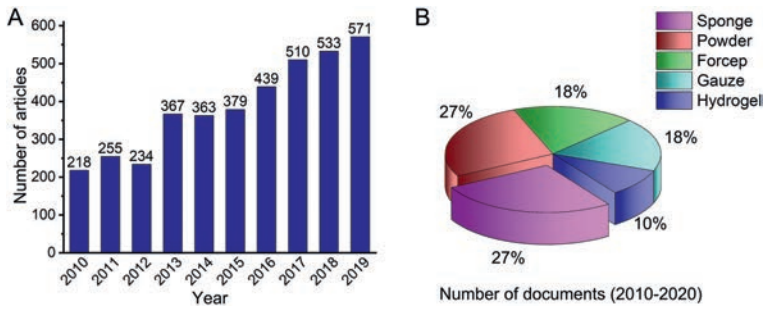

Fig. 1. (A) The development trend of the number of articles on hemostatic materials in recent ten years. (B) The types and forms of hemostatic materials in recent ten years.

Firstly, graphene oxide (GO), a derivative of graphene, has water affinity because of its oxygen-containing functional groups [40-44]. The studies reported a low-friction flow of a monolayer of water through 2D capillaries formed by closely spaced graphene sheets [45-49]. Water affinity endows GO with excellent liquid absorbability, which is similar with the passive hemostats. They can rapidly absorb plasma, enrich blood cells, platelets, coagulation factors and other mass components on the surface, so as to accelerate coagulation [50,51]. Secondly, the surface of GO-based materials is easily functionalized. It is convenient to combine with other hemostatic materials to form multifunctional hemostatic composite materials. Thirdly, graphene is a 2D lamellar structure. It is a good carrier to package coagulation stimulants, which can maintain the hemostatic performance of stimulants and prevent their disadvantages. Fourth, GO can activate platelets and trigger the coagulation cascade. Singh [52] first reported that GO nanosheet promotes platelet activation and aggregation by activating Src kinase and releasing intracellular calcium. The ability of GO to activate platelets has also been proved by other scientists [53-60]. Therefore, graphene-based materials used in the field of hemostasis have been comprehensively studied in recent years.

Based on this aspect, this review summarizes the preparation of graphene-based materials (which were prepared using GO as raw materials) and the research progress in hemostatic field for the first time, including three categories: organic cross-linked graphene sponge, inorganic composite graphene sponge, bioactive factor composite graphene sponge. The article emphasizes that the composite sponges based on GO are novel promising hemostatic materials, which provide new ideas and motivation for the research and development of hemostatic materials.

2. Graphene-based hemostatic sponge

2.1. Organic cross-linked graphene hemostatic sponge

The first reported graphene-based hemostatic material is ethylenediamine (EDA) cross-linked graphene sponge (CGS) [50]. It possessed a hierarchical porous structure with high porosity and specific surface area. The CGS [61-63] absorbed a droplet of water within 40 ms and absorbed 112 times of its own weight. When acting on the wound site, CGS quickly absorbed plasma to increase the concentration of blood cells and platelets, which will trigger the endogenous coagulation system and promote the rapid blood coagulation. Due to the fast absorption performance, CGS showed effective hemostatic performance. It stopped wound bleeding within 240 s in the tail cutting experiment of rats. As the first graphene-based material for hemostasis, CGS provides technical guidance and theoretical basis for macroscopic hemostasis of graphene. Compared with traditional hemostatic agents, CGS has many advantages, such as simple preparation, low cost, nontoxic and long shelf life. The study proposes a new hemostatic material and shows that organic cross-linked graphene materials have great potential in treating traumatic bleeding.

The hemostatic mechanism of CGS only is rapid adsorption and cannot activate blood cells or platelets because of the reduction reaction during microwave treatment. Previous study pointed out that atomically thin GO rather than reduced GO (rGO) sheets could activate platelets through the charge distribution on surface [64]. It inspired that increasing the surface charge of CGS could reinforce the interface stimulation between cells and graphene. Thus, Quan *et al.* used the medicinal amino acid 2,3-diaminopropionic acid (DapA) as cross-linker to prepare DapA cross-linked graphene sponge (DCGS, Fig. 2A) [65]. Because of the carboxyl group of DapA, the electric negative potential of DCGS increased from -18.7 ± 1.4 mV to -24.2 ± 1.3 mV. Thus, it significantly stimulated platelets and red blood cells. The platelets and red blood cells on the surface of DCGS formed pseudopodia and bonded with each other (Fig. 2B). Under the synergy of physical adsorption and charge stimulation, DCGS stopped wound bleeding within 166 s, which was 35 s less than CGS (Figs. 2C and D). The hemostatic performance of DCGS was significantly improved by the increased negative charge density on surface [66,67]. The research provides a new direction to develop graphene-based hemostatic materials by dual (or more) hemostatic mechanisms.

Nonetheless, the increased electric negative potential of DCGS was limited. The electric negative potential of GO aerogel could be up to −40.4 mV, which may further enhance the hemostatic performance. Because of the high temperature reaction and microwave action during the preparation of CGS and DCGS, the oxygen-containing functional groups on the surface of GO were reduced, which leaded to a decrease of the electric negative potential. In this regard, a mild of crosslinking strategy was proposed to preserve the oxygen-containing groups of GO during the cross-linked reaction. Polydopamine (PDA) was used as cross-linker to prepare PDA cross-linked GO sponge (DCGO) [68]. In the process, dopamine self-polymerized through an alkali-induced polymerization process and cross-linked the GO aerogel through a mild crosslinking strategy (Fig. 3A). Therefore, the oxygen-containing groups of GO were mostly reserved, and the negative potential of DCGO increased from −24.2 mV (DCGS) to –31.3 mV, showing strong platelet stimulation (Figs. 3B and C). In addition, the PDA network enhanced the mechanical strength and enabled DCGO to withstand 350 times its own weight without deformation. Strong mechanical properties insured the absorption capability of DCGO. The dynamic human blood coagulation index of DCGO was consistent with 10 units of thrombin (Fig. 3D). DCGO stopped wound bleeding within 105 ± 15 s because of the synergy of intense platelet stimulation and rapid physical absorption. DCGO combined the advantages of both PDA and GO. DCGO not only maintained the negative charge on the surface of GO, but also avoided the toxicity of GO, which maximized the hemostatic potential [69]. The study supplies a new method for preparing an effective graphene-based hemostatic material.

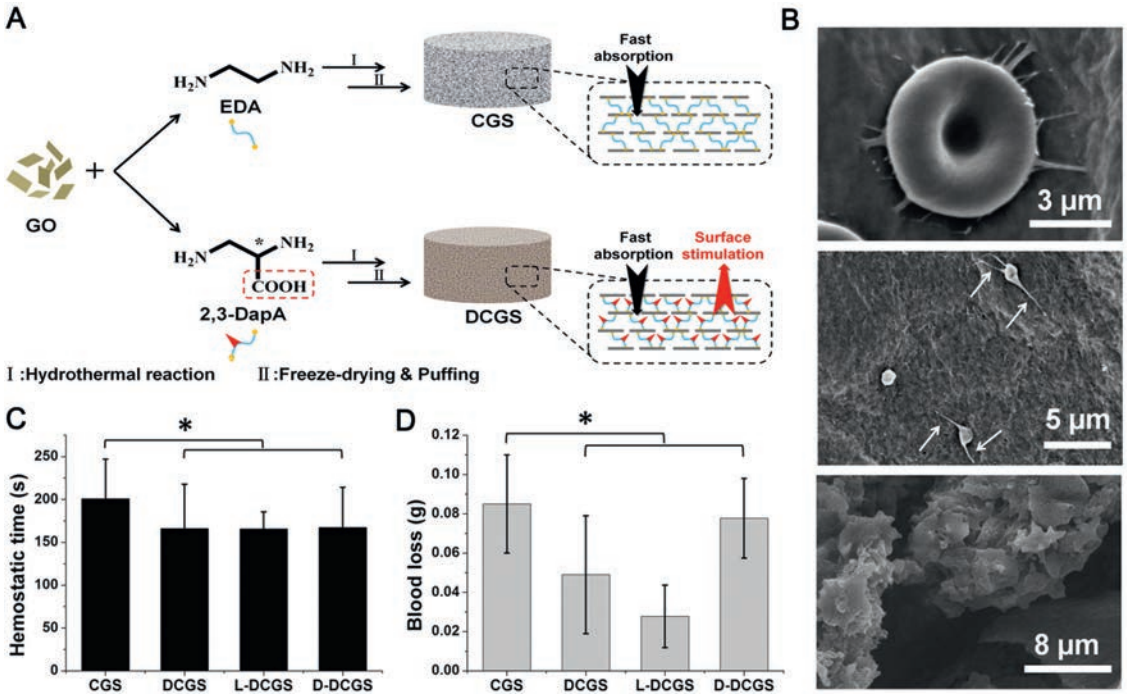

Fig. 2. (A) Schematic representation of the preparation route and the hemostatic mechanism of DCGS. (B) SEM images of interfacial interaction between blood cells and the DCGS. (C) Hemostasis time and (D) Blood loss from the rat-tail amputation model among the CGS, DCGS, L-DCGS and D-DCGS. Reproduced with permission [65]. Copyright 2016, American Chemical Society. .

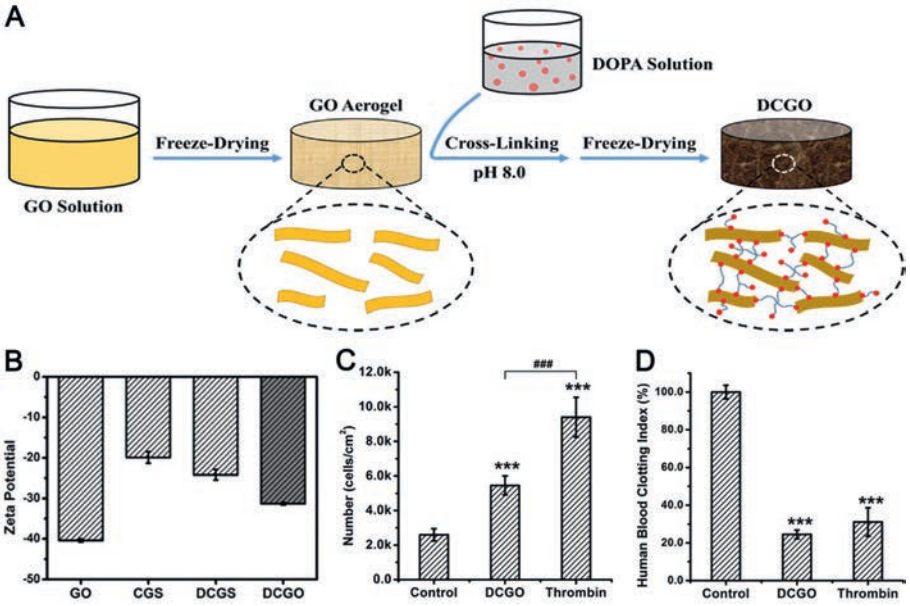

Fig. 3. (A) Schematic of the preparation of the DCGO. The un-cross-linked GO aerogel was immersed in an alkaline solution in which DOPA self-polymerized through alkali-induced polymerization and modified the surface of the GO aerogel simultaneously. After freeze-drying, the DCGO was obtained. (B) Zeta potential tests of the DCGO, GO aerogel, CGS and DCGS. (C) Statistical analysis of the number of pretreated cells adhered onto the fibrinogen matrix. (D) ACD Human blood clotting index of DCGO and thrombin (10 U). Reproduced with permission [68]. Copyright 2019, Elsevier.

Charge stimulation can effectively accelerate the clotting process. In addition to negative charges, positive charges can also promote wound coagulation. For example, positively charged chitosan can seal the wound through enriching negatively charged red blood cells and binding with negatively charged sialic acid cell on mucosa and platelets [70,71]. Zhang *et al.* combined *N*-alkylated chitosan (AC) and GO to prepare a series of AC/GO composite sponges (ACGS) through the positive and negative charge attraction and hydrogen bonding interaction (Fig. 4A) [72]. GO not only enhanced the mechanical strength and liquid adsorption performance of AC, but also increased platelet activation level and promoted the release of intracellular Ca^{2+} (Figs. 4B and C). The addition of AC endowed ACGS with positive charge, which enhanced the ability to enrich blood cells. ACGS20 with a GO ratio of 20% displayed the best blood clotting effect in rabbit femoral injury model. The hemostatic time of ACGS20 was about 134 s, and the blood loss was significantly less than GO group and AC group. At the same time, the addition of AC also improved the biocompat-

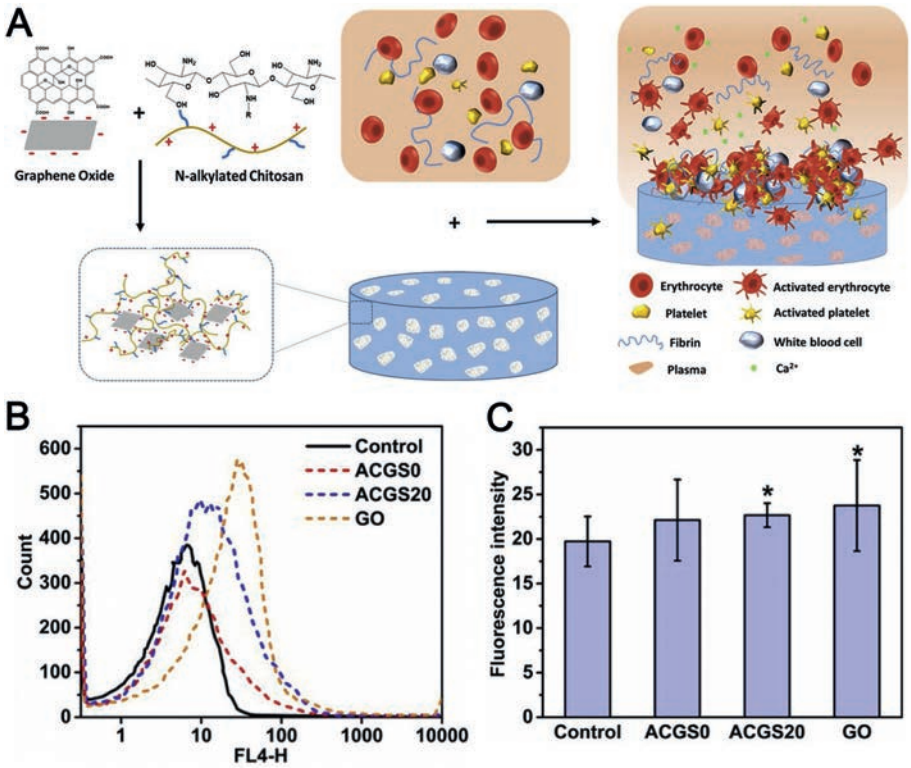

Fig. 4. (A) Schematic illustration of ACGS20 hemostasis process. Expression of (B) CD62p and (C) fluorescence intensity of intracellular Ca^{2+} in ACGS0, ACGS20, GO and control groups (* indicates $P < 0.05$ *vs.* control). Reproduced with permission [72]. Copyright 2019, Elsevier.

ibility of ACGS by reducing the hemolysis rate and cytotoxicity of GO. It is beyond doubt that ACGS shows excellent hemostatic properties by combing the advantages of both AC and GO. ACGS has considerable potential for use as an advanced hemostatic material.

Therefore, it is feasible to use EDA, DapA, PDA and AC as crosslinking agents to construct organic cross-linked graphene-based hemostatic sponges. Actually, the above crosslinking agents are mainly covalently or non-covalently linked with the active functional groups (*e.g.*, epoxy group, carboxyl group) on the surface of GO. Thus, it means that the crosslinking agents that are able to cross-link with GO can be used to construct graphene-based hemostatic sponges. The available crosslinking agents are divided into two categories. First, small molecules with active end groups, such as propylenediamine [73], glutaraldehyde [74] and ethanedithiol [75]. Second, polymers or polysaccharides, such as PVA [76], polyacrylic acid (PAA) [77], polyacrylamide (PAM) [78], functional gelatin [79] and hyaluronic acid [80]. Different cross-linkers determine the preparation methods and properties of graphene-based hemostatic sponges. Generally, the construction strategy using small molecules mainly takes GO as the main component, while that using polymers or polyacrylamides mainly takes GO as an additive to enhance mechanical strength and increase hemostatic efficiency. Additionally, active sites such as amino and carboxyl groups also could be introduced by the cross-linkers to effectively improve the electronic stimulation of the sponges and trigger the coagulation pathway. But the most important thing we believe that the basis of building this material is to ensure its biological safety while maintaining rapid liquid absorbability to improve the hemostatic performance. Considering this fact, choosing suitable cross-linker is important as its effects on the absorbability of graphene-based hemostatic sponges.

Additionally, porosity is another key factor determining the absorbability of the sponges. Effectively control the pore structure and morphology, such as pore size, structure strength and pore wall thickness, are in favor of preparing porous graphene materials. Large pores will be unable to retain blood cells and other coagulation components, while small pore reduce the liquid absorption capacity (*e.g.*, absorption weight and absorption rate). Uneven pore distribution and thin pore wall will lead to poor mechanical strength. When GO is introduced into the sponges, the pore size distribution becomes narrower; the diameter becomes smaller and the wall thickness increases obviously. Finally, the material is in a state of swelling in water for a long time without collapse [81]. Graphene-based sponge is piled by honeycomb unit structure. The formation of closely packed multi-layer structure can maximize the interaction between layers, thus greatly improving its strength and elastic stiffness [82]. It not only maintains the porous structure of the sponge, but also effectively prevents the collapse of the sponge when it is seriously compressed [83,84]. At present, porous structure of graphene-based sponge has been successfully manufactured by different methods, which can be divided into two categories: template method and template free method [85]. The materials prepared by template method have many advantages, such as high flexibility, controllable size and microstructure, and preventing agglomeration. Template method can be divided into hard template and soft template according to the composition and characteristics of template [86]. It is worth emphasizing that the ice template method, which belongs to the hard template, is one of the most concerned preparation methods [87]. In this method, the ice crystals formed in the freezing process are used as templates of porous structure to prepare porous materials. The pore structure and size can be adjusted by controlling the solute type and concentration of the solution and the rate of unidirectional freezing. Etching method [88], solution self-assembly method [89] and CVD method [90,91] are all template free methods. Template free method has strong flexibility and is more suitable for the changeable requirements of material synthesis [92,93]. Therefore, it is vital to prepare different

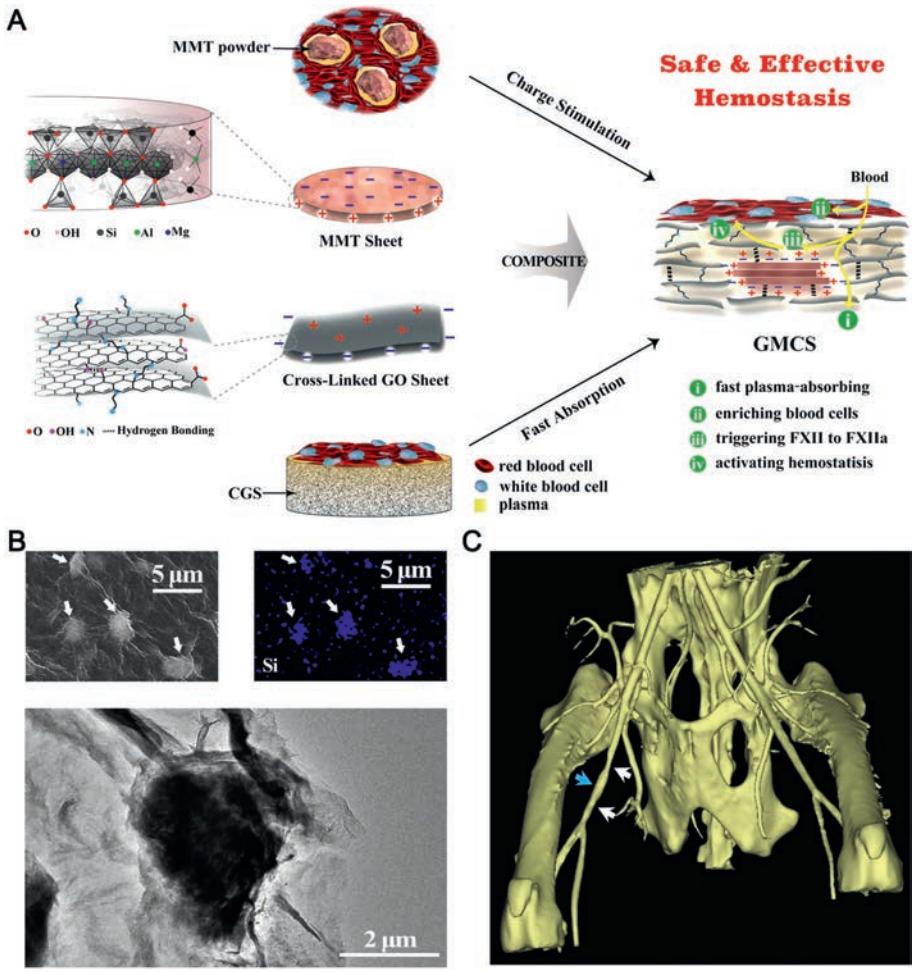

Fig. 5. (A) Schematic representation of the GMCS construction and the potential synergy effect for hemostasis. (B) SEM image of the cell wall surface (top left of image B), EDS mapping of Si elements of image (top right of image B), TEM image of the graphene-covered MMT powder (below of image B). (C) CT image of blood flow through the femoral artery 2 h after treatment. Blue arrow shows the injury site. Two white arrows denote the deformed artery caused by the forceps. Reproduced with permission [94]. Copyright 2016, American Chemical Society.

porous graphene-based sponges by different methods to improve the hemostatic performance.

2.2. Inorganic composite graphene hemostatic sponge

Inorganic clay such as montmorillonite (MMT), kaolin and zeolite has a highly effective hemostatic performance because of its strong coagulation stimulation. MMT is the most effective hemostatic clay. However, it was restricted by the Food and Drug Administration (FDA) due to the cytotoxicity and thrombus-inducing properties. Li *et al*. used graphene as a platform carrier to composite MMT to prepare graphene-MMT composite sponge (GMCS) [94]. GMCS fixed MMT particles by GO nanosheet through the perfect charge matching and hydrogen bonding interaction between MMT and GO (Figs. 5A and B). According to reports, free MMT has cytotoxic and thrombus-inducing properties, while immobilized MMT avoids the side effect. Therefore, GMCS eliminated the side effect of MMT through the immobilization. First of all, GMCS inherited the porous structure of graphene sponge, which rapidly absorbed plasma and enriched effective components such as blood cells on its surface. Second, the absorbed plasma entered the GMCS and the protein in the plasma was activated by MMT, resulting in the release of coagulation factor XIIa. Finally, MMT activated the coagulation cascade pathway to achieve rapid hemostasis. With the combined effect of physical absorption and charge stimulation, GMCS showed rapid clotting response, stopped wound bleeding within 85 s in rabbit arterial injury experiment. The total survival rate of rabbit was 100%. Importantly, GMCS did not cause thrombus. All blood vessels of the tested rabbit in CT angiography were clear and smooth (Fig. 5C). This was mainly due to the immobilization of MMT. In a word, GMCS composite sponge not only exerts the powerful hemostatic ability of MMT powder, but also eliminates its side effects. This kind of composite sponge with “win-win” effect provides a new strategy for the development of inorganic materials in the field of hemostasis.

Although GMCS eliminates the side effects of MMT, there are still worries about it. On this basis, Liang *et al*. proposed another graphene-kaolin composite sponge (GKCS) [95]. In this sponge, kaolin, a natural alum inosilicate mineral, was selected as a new stimulant to be embedded in CGS. Compared with MMT, kaolin hardly exhibits hemolysis. It will not cause harm such as cytotoxicity and hemolysis even if it enters the body freely, which shows high biocompatibility. Similar to GMCS, GKCS absorbed plasma rapidly and promoted the coagulation process. Due to the existence of a large number of negative charges, kaolin activated platelets [96]. With the activation of platelets, a series of coagulation factors were activated one by one. Finally, the GKCS promoted the cross-linked polymerization of fibrin and accelerated the coagulation process. Surprisingly, in the rabbit artery injury experiment, GKCS stopped wound bleeding in about 73 s, which showed better

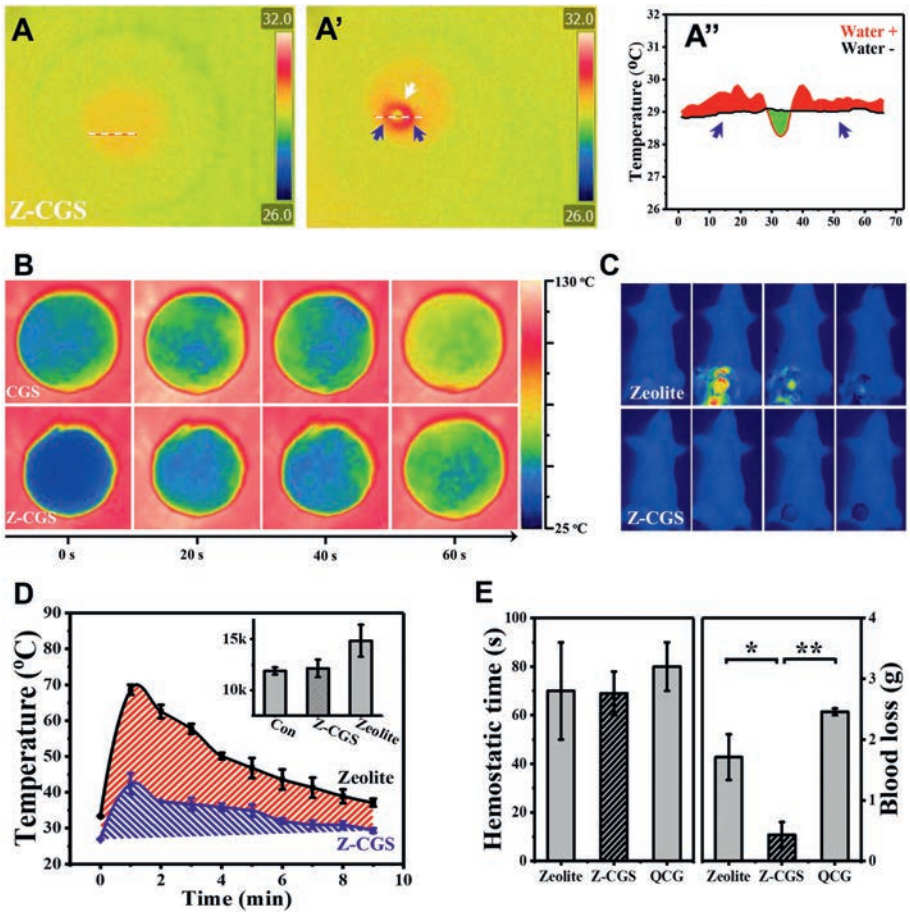

Fig. 6. (A, A') IR image and (A'') temperature curve before or after liquid absorption for the Z-CGS. (B) IR image of thermal conductivity for the CGS and the Z-CGS. (C) IR images of hemostatic process in the SD rat artery injury model by the zeolite and the Z-CGS. (D) Temperature curve of wound tissue after application of different hemostats. (E) Hemostatic time of the Z-CGS and the zeolite in the SD rat artery injury model. Reproduced with permission [98]. Copyright 2019, American Chemical Society.

hemostatic performance than GMCS. At the same time, GKCS inhibited the expression of inflammatory genes IL–1, COX–2 and IFN–γ, which was beneficial to wound healing.

As a matter of fact, zeolite is the first generation of hemostatic products with excellent hemostatic effect. However, it is gradually replaced by other hemostats because of its severe thermal damage [97]. Graphene has excellent thermal conductivity. Graphene-based sponges can conduct heat quickly to prevent heat accumulation. Thus, Liang *et al.* composited CGS with zeolite to obtain Z-CGS hemostatic sponge [98]. Z-CGS can control the heat release of zeolite and maintain stable low temperature (Figs. 6A and B). Compared with the high temperature of 70 °C caused by the exposed zeolite, Z-CGS effectively controlled the wound temperature below 42 °C (Figs. 6C and D). Thus, Z-CGS showed more significant hemostatic effects under the synergistic effect of thermal stimulation, electric charge stimulation and physical absorption capacity. The hemostatic time of Z-CGS was about 69 s, which was significantly shorter than QuikClot hemostatic gauze (80 s, Fig. 6E). Z-CGS is the first time to use the concept of ternary synergistic design, which breaks through the limitations of zeolite in hemostasis field to achieve win-win results in efficient hemostasis and biosafety. The success of Z-CGS also provides a new prospect for the development of new hemostatic agents for trauma treatment.

The above studies used three kinds of inorganic clay to improve the hemostatic performance of graphene-based sponges. It was reported that inorganic clay can absorb plasma in blood and accelerate hemostasis. However, after that, blood cells and other components gathered to wrap the clay so that it can no longer contact with plasma. Thanks to the graphene sponge, blood cells and other components were trapped on the surface of the sponge, which did not affect the liquid absorption capacity of inorganic clay. Inorganic clay was firmly fixed in the graphene sponge through a perfect charge matching mechanism. It is the key point for the preparation of the graphene/clay composite sponge. The enhancement of coagulation stimulation by inorganic clay is mainly due to its charge effect. Hemostasis is effectively mediated by surface charge. For inorganic metal oxides, it was found that the basic oxide that with isoelectric point higher than blood pH is anticoagulant (zinc oxide), while the acidic oxide that with isoelectric point lower than blood pH is coagulant (silica). For inorganic ions, according to reports, inorganic ions such as Ca^{2+} and Fe^{3+} also can interact with negatively charged blood cells and activate the blood coagulation pathway to accelerate blood clotting [99]. It is worth emphasizing that Ca^{2+} as coagulation factor IV participates in many key links of internal and external coagulation cascade in the coagulation process. It participates in regulating platelet activation and aggregation, promoting the formation of insoluble fibrin, and finally forming blood clot to prevent bleeding. Through charge effect, inorganic ions can also be compounded to enhance the mechanical strength of the graphene-based sponge [100]. Thus, it may be a feasible method to enhance the mechanical properties of the graphene-based sponge and introduce coagulation stimulation to improve the hemostatic efficiency through an inorganic composite strategy.

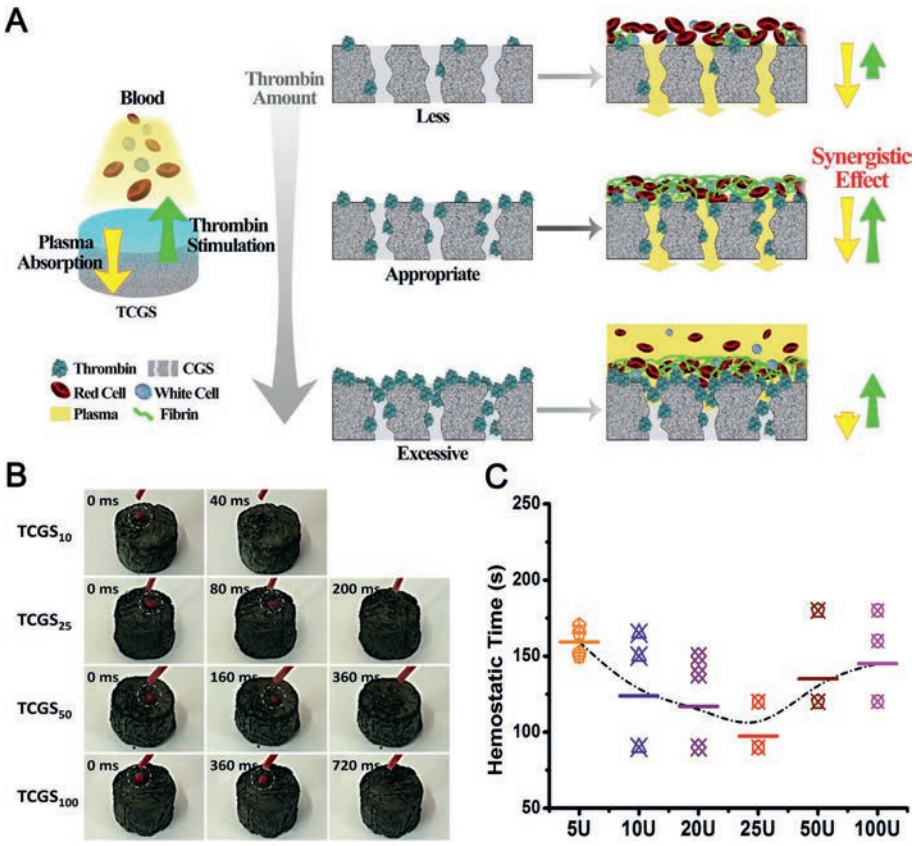

Fig. 7. (A) Schematic representation of the TCGS constructions and the synergy effect for hemostasis. The length of the yellow or green arrows represents the strength of the related performance. (B) A high-speed camera (40 ms per frame) recorded the blood absorption rate of the TCGS. $TCGS_{25}$ represents the typical TCGS. (C) The hemostatic time of the TCGS with different added amounts of thrombin (5, 10, 25, 50, 100 U). Reproduced with permission [101]. Copyright 2018, Elsevier.

2.3. Bioactive factor composite graphene hemostatic sponge

CGS is an excellent platform sponge, which can carry coagulation factors by covalent or non-covalent bonding. Li *et al.* developed thrombin/cross-linked graphene sponge (TCGS) by a spray approach [101]. Because of the abandon non-covalent interaction, thrombin strongly adhered to the GO sheets, and mainly retained on the top layer. During hemostatic process, TCGS sponge quickly absorbed blood and accelerated coagulation. Meanwhile, thrombin fixed on the surface directly contacted the plasma, and converted fibrinogen into fibrin and polymerized fibrin clot in coagulation cascade (Fig. 7A). Interestingly, because high concentration of thrombin will reduce the blood absorption capacity of the sponge and reduce the hemostatic effect, TCGS needed to achieve a balance between thrombin stimulation and plasma absorption. Only under the synergistic effect of appropriate thrombin stimulation and sponge rapid absorption, can TCGS have excellent hemostatic performance (Fig. 7B). In addition, the composite sponge had many comprehensive advantages. First of all, the porous structure of CGS ensured that thrombin was stably embedded in TCGS, and TCGS could be peeled from the wound after hemostasis finished, which not only avoided the sudden release of thrombin, but also maintained its biological activity. Secondly, for TCGS, the optimal dosage of thrombin was 25 U, which was far lower than the clinical recommended concentration of 1000 U (Fig. 7C). Low dosage of thrombin effectively reduced the cost of material preparation. TCGS could maintain good hemostatic performance even if it was kept at room temperature for six months, which was conducive to its practical application. Therefore, it is obvious that TCGS with high biosafety and stability has a broad biological prospect, and its emergence provides a new idea and strategy for the design of hemostatic materials.

Similarly, Mellado *et al.* used GO and PVA as raw materials to synthesize stable composite aerogels [102]. Natural País grape seed (SD) and peel (SK) extract enriched with proanthocyanidins (PAs) were the bioactive molecules and incorporated into the aerogel to synthesize aerogels of GO-PVA-SD and GO-PVA-SK (Fig. 8A). According to reports, PA had anti-inflammatory and antibacterial activity and can promote wound healing. The addition of PVA strengthened the 3D pore structure of aerogels and stabilized the incorporation of PA extract. Then, the incorporation of PA extract changed the content of O and C elements in the aerogel, making the negative potential of the material increased 33% (18.3 ± 1.3 mV). Therefore, GO-PVA-SD and GO-PVA-SK aerogels with high negative charge density on the surface could aggregate red blood cells in the blood and stimulate platelets, accelerating the formation of blood clot on the wound surface, which was more conducive to coagulation. In the experiment of dynamic whole blood coagulation, the clotting time was reduced by 37% and 28% during the first 30 and 60 s, which further emphasized the outstanding hemostatic performance of the aerogel. Furthermore, a stable C–O covalent bond was formed between PAs and GO-PVA, which improved the stability of the composite gel. The release time of the extract in GO-PVA-SD and GO-PVA-SK aerogels was extended to 3 h, which ensured the stable and continuous release of PAs and was beneficial to promote wound healing. However, due to the covalent bond of C–O, the release of the extract only accounted for a small part of the capture (about 14%–20%). Even so, the aerogels provide new materials and methods for trauma treatment and has great reference value.

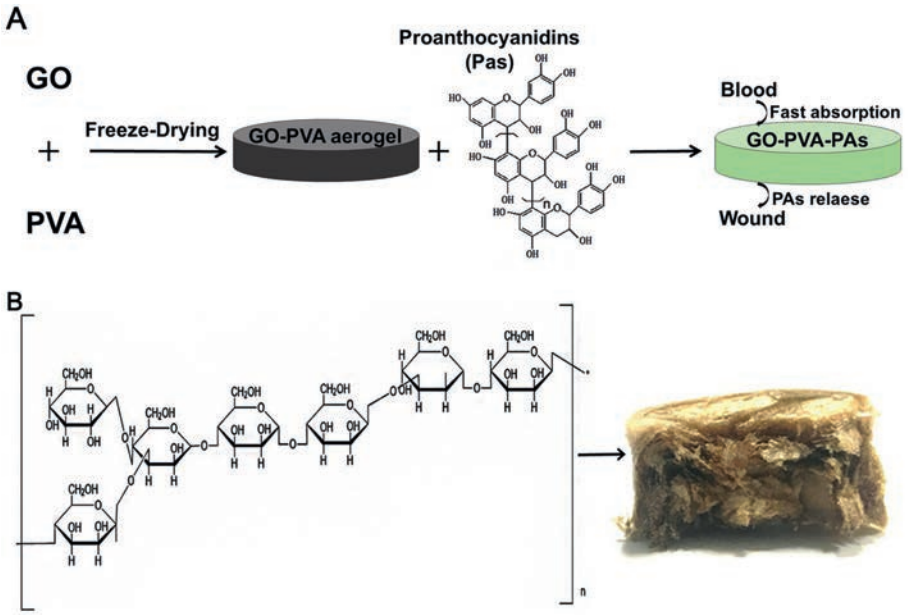

Fig. 8. (A) The preparation method and hemostasis mechanism of GO-PVA-PAs. (B) The proposed structure of the BSP, and cross section of the BGCS. Reproduced with permission [67]. Copyright 2019, Elsevier.

Based on the above strategies, Chen *et al.* used a simple solution-mixing freeze-drying method to combine Bletilla polysaccharide (BSP) with GO to prepare the BSP/GO composite sponge (BGCS) [67]. BSP is a biocompatible hemostatic drug. It has abundant hydroxyl groups and long chains, which makes it easy to cross-linked with GO (Fig. 8B). Then GO and BSP formed a stable structure through the form of hydrogen bond, which greatly improved the biocompatibility of GO. GO caused 60.9% hemolysis, while BGCS did not. Additionally, the combination of BSP and GO made BGCS have a good hemostatic ability that the hemostatic time of BGCS was 45.9 $\pm$ 4.6 s. BGCS obviously improves the potential thrombus of pure GO, and provides a new material with good biocompatibility for the field of wound hemostasis.

Graphene-based sponge is an excellent carrier, which makes it possible to compound the bioactive coagulation factor to enhance hemostatic efficiency. The factors listed in this paper include thrombin, PAs and BSP. Actually, coagulation peptide, a highly active coagulation factor, has also been widely used in the field of hemostasis. For example, amphiphilic peptide can accelerate the activation of coagulation factor X [103]. Coagulation factor X is responsible for the transformation of prothrombin to thrombin. Melittin may act on coagulation through its hemolytic effect on blood cell components (especially red blood cells and platelets) [104]. Hemolysis has also been reported to enhance thrombin production and cause a severe procoagulant state. Snake venom peptide can activate coagulation factors VIII, VII and VI, stimulate platelet aggregation, and convert prothrombin to thrombin, thus shortening fibrinogen and plasma coagulation time at the damaged vessels [105]. They can also be incorporated into CGS to obtain series of composite sponges. But in this fact, two aspects need to be considered. First, keeping the balances between peptide activation and sponge absorbability, which we were mentioned above. Second, insuring the biosafety of materials. Strong simulations of coagulation peptide may cause serious side-effects, such as thrombus and coagulation dysfunction. In order to eliminate the side-effects, it may be feasible to fix or reduce the amount of coagulation peptide. It is expected that the sponge constructed by ultra-efficiency coagulation peptide and graphene can coagulate in top speed.

3. Discussion

The advantages and disadvantages about the preparation methods of graphene-based hemostatic sponge are summarized. First, organic cross-linking method is a flexible composite strategy. The strong liquid absorption capacity of the sponges makes a big contribution to the hemostatic efficiency. But, the hemostatic stimulation is not strong enough. Second, inorganic composite method eliminates the side effects of the inorganic clay. The composite sponge greatly enhances the hemostatic efficiency by the synergistic hemostatic stimulations. But, the performance of the clay would decrease during the hydrothermal process. Third, bioactive factor composite graphene sponge would be a powerful material to achieve ultra-fast hemostasis. But, the storage conditions of the sponge depend on the added bioactive factors.

Different hemostatic materials are listed in Table 1 [50,94,95,106-118]. Compared with them, graphene-based hemostatic sponge, as an important member of the new generation hemostatic materials, has been widely recognized for its hemostatic ability and effect (Fig. 9). This mainly gives the credit to its four-latent capacity. First of all, GO has the characteristics of super affinity with water, and the porous structure of graphene-based sponge endows it with the particularity of rapid absorption of liquid. In this way, the hemostatic material based on GO can quickly absorb plasma and enrich blood cells, which is the first step in the hemostasis process. Secondly, GO is easy to be multifunctional. GO is a kind of nanosheets because of its abundant hydroxyl and epoxy groups on its surface and carboxyl functional groups on its edge. GO is easy to match with other coagulation molecules, which is the premise of the preparation of composite materials. Thirdly, the ultrafast hemostasis of graphene-based hemostatic sponge is inseparable from the synergistic effect of multiple factors. A sponge system combines different coagulation mechanisms, such as rapid adsorption, charge stimulation and even thermal stimulation, which greatly improves the hemostatic ability of the composite. In the future, it is possible to use graphene's excellent optical and electrical characteristics to achieve more diversified composite hemostasis mechanisms. Fourthly, the strategy of graphene sponge to firmly fix blood coagulation particles

Table 1
Hemostatic mechanism, advantages and disadvantages of the common used hemostats.

Hemostatic material	Hemostatic mechanism	Advantages	Disadvantages	Type	Representative products
Graphene-based sponges	Absorbs liquid, electrical stimulation, thermal stimulation	Super hydrophilicity, high water absorption, high specific surface area, good biocompatibility	Mechanical strength not strong enough	Active	CGS [50] GMCS [94] GKCS [95]
Chitosan	Electrostatic interaction with erythrocytes, accelerates red blood cell adhesion, platelet adhesion and activation	Strong adhesion, biocompatibility, biodegradability, non-toxicity, antimicrobial activity and non-antigenicity	High cost and not suitable for patients with shellfish allergy	Active	RDH [106] Celox [107] Chito Gauze Pro [108]
Kaolin	Absorbs liquid, activates platelets, activates coagulation cascade	Effective control of bleeding, no fever risk, low toxicity	No hemostatic effect in patients with coagulopathy	Active	Quikclot Combat Gauze [109]
Montmorillonite	Absorbs liquid, activates platelets, activates coagulation cascade	High specific surface area and cation exchange capacity, high viscosity	Potential risk of thrombosis	Active	Woundstat [110]
Zeolite	Absorbs liquid, activates and coagulates platelets	Low cost, stop bleeding quickly	Thermal damage to tissues	Active	QuikClot [111]
Cellulose oxide	Absorbs liquid, combines with hemoglobin iron ion, activates coagulation factor VIII and promotes platelet adhesion	Good biocompatibility, biodegradability, low toxicity, low cost	Low pH, limited in sensitive tissue applications	Passive	Xstat [112] Surgicel [113] Floseal [114]
Starch	Absorbs liquid, accelerates the natural coagulation cascade	Water-soluble, low cost, non-toxicity, biodegradable	Cannot stop serious bleeding	Passive	Arista [115]
Gelatin	Provides physical matrix for clotting initiation	Good biocompatibility, biodegradability and low cost	May cause tissue reactions	Passive	Surgifoam [116]
Collagen protein	Promotes platelet adhesion, allows coagulation factors to co-locate and activate, increases thrombin production and fibrin formation	Can be used as a scaffold for cell proliferation and accelerate wound healing	Immune risk	Active	Avitene [117]
Sodium alginate	Destroys the ionization balance of the blood, activates coagulation factor XII, absorbs liquid	High water absorption, low toxicity, good biocompatibility and biodegradability	Poor chemical stability and mechanical strength	Active	Kaltostat [118]
Thrombin	Converts fibrinogen to fibrin to form clots, activates clotting factors	Suitable for the parts that are difficult to sew or burn	Immune risk and virus contamination	Active	

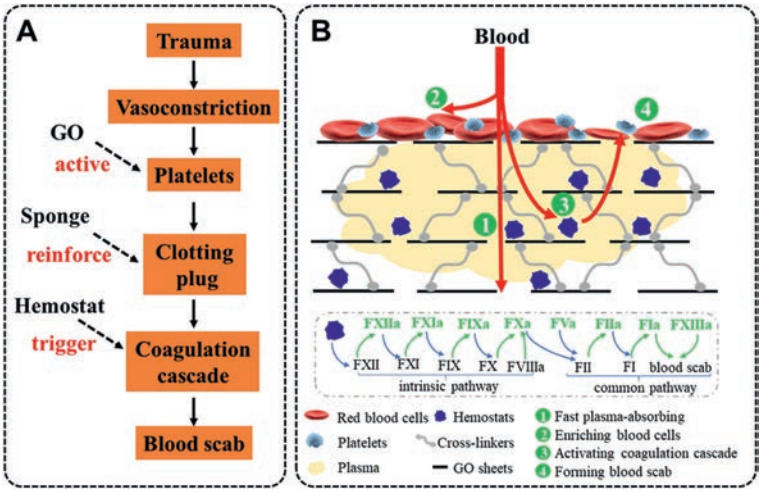

Fig. 9. The scheme of hemostatic mechanism about graphene-based sponge. (A) Contribution of graphene-based sponge in hemostasis. (B) The specific hemostatic mechanism of graphene-based sponge. Plasma in the blood is quickly absorbed into the sponge; blood cells are enriched on the surface of the sponge to form an initial clotting plug. The plasma enters into the sponge and contacts with the composite hemostats (*e.g.*, clay). Coagulation factors in the plasma are activated by hemostats and trigger coagulation cascade. Finally, fibrinogen is converted into cross-linked fibrin, which strengthens the initial clotting plug and forms blood scab to stop bleeding.

eliminates the side effects of directly acting on wound. In a word, these characteristics of graphene lay a foundation for its excellent hemostatic properties.

Although graphene-based hemostatic materials currently perform well in terms of hemostasis, there are still many challenges. First, the mechanical strength of the graphene-based hemostatic sponge is insufficient, which mainly due to the single cross-linked strategy (EDA as cross-linker), graphene sheets stacking and insufficient cross-linked sites. Thus, it may effectively improve mechanical strength of the sponge that using a variety of cross-linked methods or introducing a dual network structure. According to reports, the dual-network material has extremely high mechanical strength [119]. The construction of graphene composite sponge through the dual-network strategy, therefore, is expected

to obtain a hemostatic material with high mechanical strength. Secondly, the hemostatic properties of graphene sponge need to be further improved. A shorter hemostatic time means a higher survival rate especially in uncontrollable traumatic bleeding occurs. GO is an excellent platform carrier. The hemostatic time of graphene-based sponge is expected to be further shortened to seconds level through compounding multiple coagulation stimuli (such as charge stimulation, thermal stimulation). Under the synergistic effect of multiple coagulation stimulation, graphene-based sponge is hopeful to achieve effective hemostatic performance when treating the wound with coagulation dysfunction. Third, the multifunctional graphene-based sponge has great prospects. The composite graphene material not only has excellent hemostatic effect, but also has significant effect on promoting wound healing [120-123]. In the process of wound healing, it is easy to be infected by bacteria, which makes the wound worse and heal slowly [124-126]. Wound healing is a necessary process for wound recovery after hemostasis. Ma *et al.* prepared a flexible and microporous nanocomposite sponge SPG2-NEX by using PVA, GO and sodium alginate (SA) [127]. Norfloxacin (NFX) loaded in the composite sponge, which prevented epithelial tissue inflammation and accelerate wound healing. Li *et al.* prepared skin-regenerating hybrid membrane (*N*–Col-GO), which continuously released the antioxidant NAC [128]. The incorporation of GO reduced the gene expression related to fibrosis to prevent scar formation. Liang *et al.* incorporated rGO and antibiotic doxycycline into HA-DA hydrogel [129]. The gel showed a good effect in promoting wound healing and promoting angiogenesis. Fan *et al.* [130] proposed an Ag-graphene composite hydrogel prepared by using glucose as a green reducing agent, acrylic acid and *N,N*-methylene bis acrylamide as crosslinking agent. The porous structure of hydrogel facilitated the oxygen exchange of wound tissue cells, maintained suitable water environment, and promoted wound tissue regeneration. Additionally, secondary bleeding caused by material peeling is not expected for hemostatic materials. Adhesion difference of hemostatic materials on tissue and blood scab is an effective strategy for avoiding secondary bleeding. Graphene-based sponge is a good carrier, and the adhesion difference may be achieved through a composite strategy, which can effectively regulate the composition. Therefore, this may also be a development direction for the multifunctional of graphene-based sponges.

4. Conclusion

In summary, we reviewed the research progress of graphene-based hemostatic sponges, including three different preparation approaches (organic cross-linking, inorganic composite and bioactive factor addition) and their hemostatic mechanism. Graphene-based hemostatic sponges possess unique advantages, such as super hydrophilicity, rapid liquid absorption, platelet stimulation and good biocompatibility. In addition, graphene-based hemostatic sponges are versatile platform and could be multi-functional by flexible composite strategies. We anticipate that graphene-based hemostatic materials will have great potential for application in the field of trauma.

Declaration of competing interest

The authors declare no competing financial interest.

Acknowledgements

G. Li thanks the National Natural Science Foundation of China (No. 22005020) for the financial support.

References

[1] L.W. Chan, X. Wang, H. Wei, et al., Sci. Transl. Med. 7 (2015) 277ra29.
[2] A.M. Behrens, M.J. Sikorski, P. Kofinas, J. Biomed. Mater. Res. A 102 (2014) 4182–4194.
[3] P. Hangge, J. Stone, H. Albadawi, et al., Cardiovasc. Diagn. Ther. 7 (2017) S267.
[4] L.W. Chan, C.H. Kim, X. Wang, et al., Acta Biomater. (2016) 178–185.
[5] Y. Li, H. Li, L. Xiao, et al., Materials (Basel) 5 (2012) 2586–2596.
[6] X. Yang, W. Liu, N. Li, et al., Biomater. Sci. 5 (2017) 2357–2368.
[7] M. Emilia, S. Luca, B. Francesca, et al., Transfus. Apher. Sci. 45 (2011) 305–311.
[8] P. Nakielski, F. Pierini, Acta Biomater. 84 (2019) 63–76.
[9] D.A. Hickman, C.L. Pawlowski, U.D. Sekhon, J. Marks, A.S. Gupta, Adv. Mater. 30 (2018) 1700859.
[10] H.E. Güven, Ulus Travma. Acil. Cer. 23 (2017) 357–361.
[11] S. Pourshahrestani, E. Zeimaran, I. Djordjevic, N.A. Kadri, M.R. Towler, Mater. Sci. Eng. C 58 (2016) 1255–1268.
[12] X.X. Wang, Q. Liu, J.X. Sui, et al., Adv. Healthc. Mater. 8 (2019) 1900823.
[13] Y. Chen, L. Wu, P. Li, et al., Macromol. Biosci. 20 (2020) 1900370.
[14] V. Mittal, Macromol. Mater. Eng. 299 (2014) 906–931.
[15] L. Ma, M. Zhou, C. He, et al., Green Chem. 21 (2019) 4887–4918.
[16] V. Dhand, K.Y. Rhee, H. Ju Kim, D. Ho Jung, J. Nanomater. (2013) 763953.
[17] Q. Tang, Z. Zhou, Z. Chen, Nanoscale 5 (2013) 4541–4583.
[18] D. Ege, A.R. Kamali, A.R. Boccaccini, Adv. Eng. Mater. 19 (2017) 1700627.
[19] S.K. Tiwari, S. Sahoo, A. Huczko, J. Sci. Adv. Mater. Dev. 5 (2020) 10–29.
[20] C. Chung, Y.K. Kim, D. Shin, et al., Acc. Chem. Res. 46 (2013) 2211–2224.
[21] A. Gulzar, P. Yang, F. He, et al., Chem. Br. Interact. 262 (2017) 69–89.
[22] T.A. Esquivel-Castro, M. Ibarra-Alonso, J. Oliva, A. Martínez-Luévanos, Sci. Eng. C 96 (2019) 915–940.
[23] A. Madni, S. Noreen, I. Maqbool, et al., J. Drug Target. 26 (2018) 858–883.
[24] S. Kumar, K. Chatterjee, ACS Appl. Mater. Interfaces 8 (2016) 26431–26457.
[25] A.N. Banerjee, Interface Focus 8 (2018) 20170056.
[26] S. Kumar, C. Gautam, V.K. Mishra, et al., ACS Omega 4 (2019) 7448–7458.
[27] T.P.D. Shareena, D. McShan, A.K. Dasmahapatra, P.B. Tchounwou, Nanomicro. Lett. 10 (2018) 53.
[28] G. Reina, J.M. González-Domínguez, A. Criado, et al., Chem. Soc. Rev. 46 (2017) 4400–4416.
[29] S. Goenka, V. Sant, S. Sant, J. Control Release 173 (2014) 75–88.
[30] H. Ji, H. Sun, Adv. Drug Deliv. Rev. 105 (2016) 176–189.
[31] S. Sayyar, D.L. Officer, G.G. Wallace, J. Mater. Chem. B 5 (2017) 3462–3482.
[32] A. Idowu, B. Boesl, A. Agarwal, Carbon 135 (2018) 52–71.
[33] O. Akhavan, J. Mater. Chem. B 4 (2016) 3169–3190.
[34] Q. Fang, Y. Shen, B. Chen, Chem. Eng. J. 264 (2015) 753–771.
[35] C. Li, G. Shi, Nanoscale 4 (2012) 5549–5563.
[36] M.A. Worsley, P.J. Pauzauskie, T.Y. Olson, et al., J. Am. Chem. Soc. 132 (2010) 14067–14069.
[37] M. Pumera, Chem. Soc. Rev. 39 (2010) 4146–4157.
[38] E. Cuce, P.M. Cuce, C.J. Wood, S.B. Riffat, Renew. Sust. Energ. Rev. 34 (2014) 273–299.
[39] V. Chabot, D. Higgins, A. Yu, et al., Energy Environ. Sci. 7 (2014) 1564–1596.
[40] A. Darbandi, E. Gottardo, J. Huff, M. Stroscio, T. Shokuhfar, JOM 70 (2018) 566–574.
[41] J. Liu, J. Dong, T. Zhang, Q. Peng, J. Control Release 286 (2018) 64–73.
[42] H.M. Hegab, L.D. Zou, ACS Appl. Mater. Interfaces 484 (2015) 95–106.
[43] G. Li, S. Ma, H. Yang, et al., AICHE J. 66 (2020) e16753.
[44] W. Li, L. Zhang, X. Zhang, et al., J. Membr. Sci. 596 (2020) 117744.
[45] P. Liu, C.T. Zhu, A.P. Mathew, J. Hazard. Mater. 371 (2019) 484–493.
[46] L.Z. Guan, J. Patiño, C. Cuadrado-Collados, et al., ACS Appl. Mater. Interfaces 11 (2019) 24493–24503.
[47] A. Lerf, A. Buchsteiner, J. Pieper, S. Schöttl, I. Dekany, et al., J. Phys. Chem. Solid 67 (2006) 1106–1110.
[48] R. Nair, H. Wu, P. Jayaram, I. Grigorieva, A. Geim, Science 335 (2012) 442–444.
[49] X. Sui, H. Ding, Z. Yuan, et al., Carbon 148 (2019) 277–289.
[50] K. Quan, G. Li, D. Luan, et al., Colloids Surf. B 132 (2015) 27–33.
[51] K. Quan, G. Li, L. Tao, et al., ACS Appl. Mater. Interfaces 8 (2016) 7666–7673.
[52] S.K. Singh, M.K. Singh, M.K. Nayak, et al., ACS Nano 5 (2011) 4987–4996.
[53] B. Cai, K. Hu, C. Li, J. Jin, Y. Hu, Appl. Surf. Sci. 356 (2015) 844–851.
[54] R. Feng, Y. Yu, C. Shen, Y. Jiao, C. Zhou, J. Biomed Mater. Res. A 103 (2015) 2006–2014.
[55] Kenry, J. Mater. Res. 33 (2018) 44–57.
[56] S. Kumari, M.K. Singh, S.K. Singh, J.J. Grácio, D. Dash, Nanomedicine 9 (2014) 427–440.
[57] G. Li, Y. Liang, C. Xu, et al., Colloids Surf. B 174 (2019) 35–41.
[58] S.K. Singh, M.K. Singh, P.P. Kulkarni, et al., ACS Nano 6 (2012) 2731–2740.
[59] P. Wilczek, R. Major, L. Lipinska, J. Lackner, A. Mzyk, Mater. Sci. Eng. C 53 (2015) 310–321.
[60] Y. Zhang, J. Guan, J. Wu, et al., Carbohydr. Polym. 219 (2019) 405–413.
[61] Z. Liu, Y. Hao, Y. Su, et al., Korean J. Mater. Res. 34 (2019) 490–499.
[62] Z. Zhang, G. Kuang, S. Zong, et al., Adv. Mater. 30 (2018) 1803217.
[63] Y. Wang, C. Wang, L. Qiao, et al., Appl. Mater. Today 13 (2018) 228–241.
[64] S.K. Singh, M.K. Singh, M.K. Nayak, et al., ACS Nano 5 (2011) 4987–4996.
[65] K. Quan, G. Li, L. Tao, et al., ACS Appl. Mater. Interfaces 8 (2016) 7666–7673.
[66] Z. Zhai, K. Xu, L. Mei, et al., Soft Matter 15 (2019) 8603–8610.
[67] J. Chen, L. Lv, Y. Li, et al., Int. J. Biol. Macromol. 130 (2019) 827–835.
[68] G. Li, Y. Liang, C. Xu, et al., Colloids Surf. B 174 (2019) 35–41.
[69] X.X. Wang, Q. Liu, J.X. Sui, et al., Adv. Healthc. Mater. 8 (2019) 1900823.
[70] J. Yang, F. Tian, Z. Wang, et al., ACS Appl. Bio Mater. 84 (2008) 131–137.

[71] J. Granville-Chapman, N. Jacobs, M.J. Midwinter, Injury 42 (2011) 447–459.
[72] Y. Zhang, J. Guan, J. Wu, et al., Carbohydr. Polym. 219 (2019) 405–413.
[73] H. Hu, Z. Zhao, W. Wan, Y. Gogotsi, J. Qiu, Adv. Mater. 25 (2013) 2219–2223.
[74] A.Z. Moghaddam, E. Esmaeilkhanian, M. Shakourian–Fard, Int. J. Biol. Macromol. 128 (2019) 61–73.
[75] L. Hu, D.B. Li, L. Gao, et al., Adv. Funct. Mater. 26 (2016) 1899–1907.
[76] H.J. Salavagione, M.A. Gomez, G. Martinez, Macromolecules 42 (2009) 6331–6334.
[77] Y. Lin, L. Cao, Z. Yu, et al., SM&T 26 (2020) e00223.
[78] L. Pan, X. Fei, L. Yang, et al., Mater. Des. 202 (2021) 109587.
[79] S. Guajardo, T. Figueroa, J. Borges, et al., J. Inorg. Organomet. P. 31 (2021) 1517–1526.
[80] Q. Wang, W. She, X. Lu, et al., Comput. Theor. Chem. 1165 (2019) 112559.
[81] W. Cui, J. Ji, Y.F. Cai, H. Li, R. Ran, J. Mater. Chem. A 3 (2015) 17445–17458.
[82] S. Mo, J. Mei, Q. Liang, Z. Li, Chemosphere 271 (2021) 129827.
[83] P. Choudhary, B. Ramalingam, S.K. Das, ACS Biomater. Sci. Eng. 6 (2020) 5911–5929.
[84] X. Zhao, M. Zhou, Q. Peng, et al., Adv. Eng. Mater. 22 (2020) 2000231.
[85] H. Jahandideh, Q.A. Nguyen, N. TufenkjiInterfaces, ACS Appl. Mater. Inter. 12 (2020) 52095–52103.
[86] X. Hu, L. Yan, Y. Wang, M. Xu, Carbohydr. Polym. 258 (2021) 117622.
[87] P. Yang, G. Tontini, J. Wang, I.A. Kinloch, S. Barg, Nanotechnology 32 (2021) 205601.
[88] Z. Huang, N. Geyer, P. Werner, J. De Boor, U. Gösele, Adv. Mater. 23 (2011) 285–308.
[89] L.J. Dai, Acc. Chem. Res. 46 (2013) 31–42.
[90] H.T. Chin, H.T. Nguyen, S.H. Chen, et al., 2D Mater. 8 (2021) 035016.
[91] W. Tao, S. Zeng, Y. Xu, et al., Compos. Part A Appl. Sci. Manuf. 143 (2021) 106293.
[92] R. Bentini, A. Pola, L.G. Rizzi, A. Athanassiou, D. Fragouli, Chem. Eng. J. 372 (2019) 1174–1182.
[93] S. Zhang, W. Yang, Y. Liang, et al., Appl. Catal. B 285 (2021) 119780.
[94] G. Li, K. Quan, Y. Liang, et al., ACS Appl. Mater. Interfaces 8 (2016) 35071–35080.
[95] Y. Liang, C. Xu, G. Li, et al., Colloids Surf. B 169 (2018) 168–175.
[96] M. Long, B. Zhang, S. Peng, et al., Mater. Sci. Eng. C 105 (2019) 110081.
[97] H. Chen, X.Q. Shang, L.S. Yu, L.P. Xiao, J. Fan, J. Biomater. Appl. 34 (2020) 988–997.
[98] Y. Liang, C. Xu, F. Liu, et al., ACS Appl. Mater. Interfaces 11 (2019) 23848–23857.
[99] T.A. Ostomel, Q. Shi, P.K. Stoimenov, G.D. Stucky, Langmuir 23 (2007) 11233–11238.
[100] H.P. Cong, P. Wang, S.H. Yu, Small 10 (2014) 448–453.
[101] G. Li, K. Quan, C. Xu, et al., Colloids Surf. B 161 (2018) 27–34.
[102] C. Mellado, T. Figueroa, R. Báez, et al., ACS Appl. Mater. Interfaces 10 (2018) 7717–7729.
[103] J. Wu, C.A. Lemarié, J. Barralet, M.D. Blostein, Acta Biomater. 9 (2013) 9194–9200.
[104] H.T. Peng, H. Huang, P.N. Shek, et al., J. Bioact. Compat. Polym. 25 (2010) 75–97.
[105] V.A. Kumar, N.C. Wickremasinghe, S. Shi, J. Hartgerink, ACS Biomater. Sci. Eng. 1 (2015) 1300–1305.
[106] D.D. Jewelewicz, S.M. Cohn, B.A. Crookes, K.G. Proctor, J. Trauma 55 (2003) 275–280.
[107] H. Amoozgar, S. Abtahi, M.R. Edraki, et al., Iran. J. Pediatr. 30 (2020) 6.
[108] I. Otrocka-Domagala, P. Jastrzebski, Z. Adamiak, et al., Pol. J. Vet. Sci. 19 (2016) 337–343.
[109] D. Johnson, M. Johnson, Am. J. Emerg. Med. 14 (2019) 17–23.
[110] H. Lydon, C. Hall, H. Matar, et al., J. Appl. Toxicol. 38 (2018) 318–328.
[111] J. Li, W. Cao, L. Jiang, et al., ACTA Pharmacol. 34 (2013) 367–372.
[112] A.M. Bonanno, T.L. Graham, L.N. Wilson, J.D. Ross, PLoS One 15 (2020) e0241906.
[113] M.H. MacDonald, A.Y. Wang, J.W. Clymer, R.W. Hutchinson, R. Kocharian, Med. Devices 10 (2017) 273–279.
[114] Q. Bonduelle, T.C. Biggs, F. Sipaul, Clin. Otolaryngol. 45 (2020) 960–962.
[115] T. Altintas, N.B.D. Onalan, M.C. Kizilkaya, N. Gunduz, M.A. Bozkurt, Acta Chir. Belg. (2021) 1–8.
[116] A. Shukla, J.C. Fang, S. Puranam, P.T. Hammond, J. Control Release 157 (2012) 64–71.
[117] B.E. Evans, N. Y. Dent. J. 44 (1978) 441–443.
[118] M.I. Nelea, L. Paelz, L. Dao, et al., Burns 45 (2019) 1122–1130.
[119] J.P. Gong, Y. Katsuyama, T. Kurokawa, Y. Osada, Adv. Mater. 15 (2003) 1155–1158.
[120] W. Huang, G.C. Tsui, C. Tang, M. Yang, Compos. B. Eng. 95 (2016) 272–281.
[121] Y. Li, T. Jing, G. Xu, et al., Polymer (Guildf) 149 (2018) 13–22.
[122] Y. Qian, Y. Yuan, H. Wang, et al., J. Mater. Chem. A 6 (2018) 24676–24685.
[123] T. Kaur, A. Thirugnanam, K. Pramanik, Mater. Today Commun 12 (2017) 34–42.
[124] O. Castano, S. Pérez-Amodio, C. Navarro-Requena, M.Á. Mateos-Timoneda, E. Engel, Adv. Drug Deliv. Rev. 129 (2018) 95–117.
[125] X. Zhao, H. Wu, B. Guo, et al., Biomaterials 122 (2017) 34–47.
[126] X. Zhao, B.L. Guo, H. Wu, Y.P. Liang, P.X. Ma, Nat. Commun. 9 (2018) 1–17.
[127] R. Ma, Y. Wang, H. Qi, et al., Compos. B. Eng. 167 (2019) 396–405.
[128] J. Li, C. Zhou, C. Luo, et al., Theranostics 9 (2019) 5839.
[129] Y. Liang, X. Zhao, T. Hu, et al., Small 15 (2019) 1900046.
[130] Z. Fan, B. Liu, J. Wang, et al., Adv. Funct. Mater. 24 (2014) 3933–3943.